Electronic Supplementary Information

A Comparative Study of a Fluorene-based Non-fullerene Electron Acceptor and $PC_{61}BM$ in Organic Solar Cell-at Quantum Chemical Level

Qing-Qing Pan,[a] Shuang-Bao Li,[a] Yong Wu,[b] Guang-Yan Sun,[c] Yun Geng*[a], and Zhong-Min Su*a

[a.] *Institute of Functional Material Chemistry, Faculty of Chemistry, Northeast Normal University, Chang Chun 130024, Jilin, P. R. China. E-mail: gengy575@nenu.edu.cn; zmsu@nenu.edu.cn*

[b.] *School of Pharmaceutical Sciences, Changchun University of Chinese Medicine, 1035 Boshuo Road, Changchun, 130117, PR China*

[c.] *Department of Chemistry, Faculty of Science, Yanbian University, Yanji, Jilin, 133002, China.*

Contents

Computational methods and model

1 The interface geometry model

Regarding the electronic couplings from eq 2, except for ΔE and μ_{tr}, we calculated $\Delta\mu$ by using a finite field method on the transition excitation energy, which can be expressed as[1, 2]

$$E_{\mathrm{EXC}}(F) = E_{\mathrm{EXC}}(0) - \Delta\mu F - 0.5\Delta\alpha F^2 \quad \text{(S1)}$$

Where F is the static electric field, E_{EXC} and $\Delta\alpha$ are the excitation energy at zero field and the change in the polarizability, respectively. $\Delta\mu$ is the dipole moment difference between the initial and the final state. The excitation energy of the D/A interface were calculated based on the TD-DFT theory with CAM-B3LYP functional and 6-31G(d, p) basis set.

Generally, for exciton, the electron and the hole often experience a strong attraction, which is called exciton binding energy (E_b).[3] The E_b has to be overcome for the charges to escape from the D/A interface and migrate towards the cathode and the anode.

$$E_b = \Delta E_{\text{H-L}} - E_{S1} \quad \text{(S2)}$$

$\Delta E_{\text{H-L}}$ is the energy difference between HOMO and LUMO, and E_{S1} is the first singlet excitation energy of acceptor. Based on this formulation, we calculated E_b at the B3LYP/6-31G(d, p) level.

The reorganization energy λ is normally decomposed into internal energy (λ_i) and external energy (λ_s). The internal reorganization energy can be estimated from the exciton dissociation and charge recombination processes[4]. The reorganization energy of the charge dissociation, $\lambda_{\text{i-CS}}$, can be estimated according to the eq. (S3-S5):

$$\lambda_{i1} = \left[E^{D^*}(Q_P) + E^{A}(Q_P)\right] - \left[E^{D^*}(Q_R) + E^{A}(Q_R)\right] \quad \text{(S3)}$$

$$\lambda_{i2} = \left[E^{D^+}(Q_R) + E^{A^-}(Q_R)\right] - \left[E^{D^+}(Q_P) + E^{A^-}(Q_P)\right] \quad \text{(S4)}$$

$$\lambda_{\text{i-CS}} = (\lambda_{i1} + \lambda_{i2})/2 \quad \text{(S5)}$$

The reorganization energy of the charge recombination process, $\lambda_{\text{i-CR}}$, is given by:

$$\lambda_{i2} = \left[E^{D^+}(Q_R) + E^{A^-}(Q_R)\right] - \left[E^{D^+}(Q_P) + E^{A^-}(Q_P)\right] \quad \text{(S6)}$$

$$\lambda_{i3} = \left[E^{D}(Q_R) + E^{A}(Q_R)\right] - \left[E^{D}(Q_P) + E^{A}(Q_P)\right] \quad \text{(S7)}$$

$$\lambda_{\text{i-CR}} = (\lambda_{i2} + \lambda_{i3})/2 \quad \text{(S8)}$$

Where λ_{i1} represents the difference between the energy of the excited-state (D*A) reactants in the geometry characteristic of the products and that in their equilibrium geometry, λ_{i2} is the difference between the energy of the ionic-state (D^+A^-) reactants in the geometry characteristic of the reactants and that in their equilibrium geometry, λ_{i3} is the difference between the energy of the ground-state (DA) reactants in the characteristic of the products and that in their equilibrium geometry. Q_P and Q_R are the equilibrium geometries of the products and reactants, respectively.

In the interface model, external reorganization energy accounts for an important fraction of λ, and can't been ignored. The calculation of external reorganization energy λ_s is based on the classical dielectric continuum model[5] with the quantum mechanics methods[6] and it is given by

$$\lambda_s = \Delta q^2 \left(\frac{1}{2d_D} + \frac{1}{2d_A} - \frac{1}{d_{DA}}\right)\left(\frac{1}{\epsilon_{op}} - \frac{1}{\epsilon_o}\right) \quad \text{(S9)}$$

Where d_{DA} represents the mass-center distance between the donor and the acceptor, d_D and d_A are the radii of the donor and acceptor, respectively. ϵ_{op} is the optical-frequency dielectric constant and ϵ_o is the zero-frequency dielectric constant of the medium.

2 The calculation of electron mobility

The electron mobility can be represented as

$$\mu = eD/k_B T \tag{S10}$$

Where e is defined as the electronic charge and D is defined as the diffusion coefficient which can be approximately evaluated as[7, 8]

$$D = \frac{1}{2n}\sum_i r^2 k_i P_i \tag{S11}$$

Where n (n=3) is defined as the dimensionality, r is defined as the charge hopping centroid-to-centroid distance and k_i is the hopping rate due to charge carrier to the ith neighbor. P_i is the relative probability for charge to a particular ith neighbor

$$P_i = \frac{k_i}{\sum_i k_i} \tag{S12}$$

The intermolecular hopping rate could be described by Marcus theory[9, 10]

$$k = \frac{2\pi}{h\sqrt{4\pi\lambda k_B T}} V^2 \exp\left(-\frac{\lambda}{4k_B T}\right) \tag{S13}$$

Where V is defined as the transfer integral, T is the temperature (300K), and k and $\hbar$ are the Boltzmann and Planck constants, respectively.

Generally, the λ consists of contributions from the internal and external reorganization[11, 12]. The external reorganization is small in the carrier transmission process of crystal or amorphous thin film that can be neglected[13]. The internal reorganization, λ_i, can be easily calculated from the adiabatic potential energy surface curve method

$$\lambda_i = \lambda_- + \lambda_0 = \left[E^-(M) - E^-(M^-)\right] + \left[E(M^-) - E(M)\right] \tag{S14}$$

λ_0 is defined as the relaxation energy from the neutral molecule in its equilibrium geometry to the relaxed geometry of the ion. λ_- is defined as the relaxation energy from the ionic molecule in its relaxed geometry to the equilibrium geometry of the neutral. *E-(M)* and *E(M)* are the energies of the anion and the neutral molecule with the optimized geometry of the neutral geometries, respectively. $E^-(M^-)$ and $E(M^-)$ are the energies of the anion and the neutral molecule with the optimized of the anion geometries, respectively.

The effective transfer integral represents the strength of neighboring intermolecular electronic coupling and was evaluated by the site energy corrected method:[14]

$$V_{12}^{\text{eff}} = \frac{V_{12} - \frac{1}{2}(\varepsilon_1 + \varepsilon_2)S_{12}}{1 - S_{12}^2} \tag{S15}$$

Where $S_{12} = \langle \psi_1 | \psi_2 \rangle$ is defined as overlap integral, $\varepsilon_i = \langle \psi_i | H | \psi_i \rangle$ is the site-energy and $V_{12} = \langle \psi_1 | H | \psi_2 \rangle$ is transfer integral. We assume that H is the Hamiltonian of the dimer, ψ_1 and ψ_2 are the lowest unoccupied molecular orbitals (LUMOs) and the highest occupied molecular orbitals (HOMOs) of the two monomers.

Table S1. Calculated and experimental bond lengths (in Å), bond angles (in deg) and torsion angles (in deg) of **FENIDT** at S_0 state.

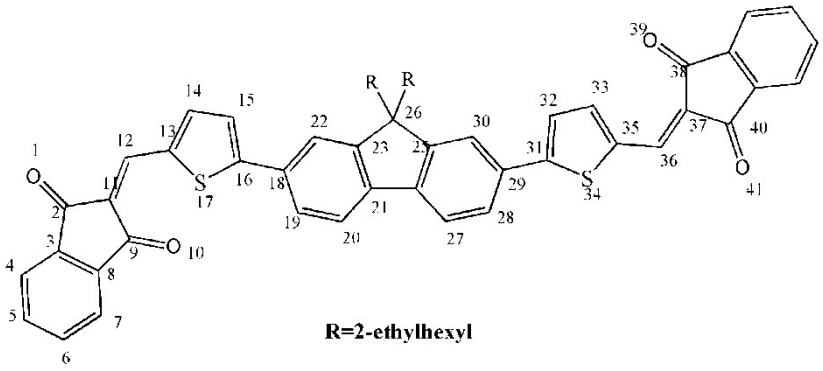

	FENIDT			FENIDT	
	Cal.	Exp.		Cal.	Exp.
			Bond Length (Å)		
R(1,2)	1.222	1.214	R(22,23)	1.385	1.382
R(2,3)	1.495	1.481	R(21,23)	1.411	1.403
R(3,4)	1.391	1.390	R(23,24)	1.529	1.524
R(4,5)	1.398	1.377	R(24,25)	1.529	1.525
R(5,6)	1.404	1.385	R(25,26)	1.411	1.395
R(6,7)	1.398	1.384	R(21,26)	1.462	1.465
R(7,8)	1.391	1.382	R(26,27)	1.397	1.385
R(3,8)	1.402	1.389	R(27,28)	1.391	1.384
R(8,9)	1.497	1.491	R(28,29)	1.411	1.401
R(9,10)	1.226	1.219	R(29,30)	1.413	1.407
R(9,11)	1.478	1.467	R(25,30)	1.384	1.377
R(2,11)	1.491	1.488	R(29,31)	1.463	1.457
R(11,12)	1.363	1.358	R(31,32)	1.330	1.371
R(12,13)	1.426	1.428	R(32,33)	1.405	1.379
R(13,14)	1.394	1.380	R(31,34)	1.741	1.708
R(14,15)	1.402	1.399	R(34,35)	1.763	1.733
R(15,16)	1.389	1.381	R(33,35)	1.392	1.368
R(16,17)	1.746	1.720	R(35,36)	1.426	1.428
R(13,17)	1.760	1.734	R(36,37)	1.366	1.364
R(16,18)	1.460	1.465	R(37,38)	1.483	1.482
R(18,19)	1.411	1.403	R(38,39)	1.227	1.216
R(19,20)	1.390	1.380	R(37,40)	1.494	1.474
R(20,21)	1.397	1.392	R(40,41)	1.222	1.211
R(18,22)	1.413	1.406			
			Bond Angle (deg)		
A(2,11,12)	120.634	120.372	A(28,29,31)	121.275	122.125
A(11,12,13)	133.405	133.273	A(29,31,34)	121.910	122.581
A(12,13,17)	127.626	127.092	A(34,35,36)	118.081	131.751
A(17,16,18)	121.311	121.340	A(35,36,37)	131.762	131.471
A(16,18,19)	121.151	121.261	A(36,37,38)	129.259	131.823

Torsion Angle (deg)					
D(17,16,18,19)	-24.230	-24.196	D(28,29,31,34')	23.248	17.181

a) Abbreviations: R = bond length, A = bond angle, D = torsion angle.

Table S2. Calculated the total reorganization energy λ_{CS} (eV) and λ_{CR} (eV), Gibbs free energy change ΔG_{CS} (eV) and ΔG_{CR} (eV), and rates k_{CS} (s^{-1}) and k_{CR} (s^{-1}) of **P3HT/FENIDT-style1** interface

	λ_{CS}	λ_{CR}	ΔG_{CS}	ΔG_{CR}	k_{CS}	k_{CR}
P3HT/FENIDT-style1	0.59	0.63	-0.85	-1.60	9.01×10^{14}	1.44×10^{9}

Table S3. Calculated the total reorganization energy λ_{CS} (eV) and λ_{CR} (eV), Gibbs free energy change ΔG_{CS} (eV) and ΔG_{CR} (eV), and rates k_{CS} (s^{-1}) and k_{CR} (s^{-1}) of **P3HT/3** interface

	λ_{CS}	λ_{CR}	ΔG_{CS}	ΔG_{CR}	k_{CS}	k_{CR}
P3HT/3	0.49	0.52	-0.58	-1.96	7.64×10^{15}	0.10×10^{0}

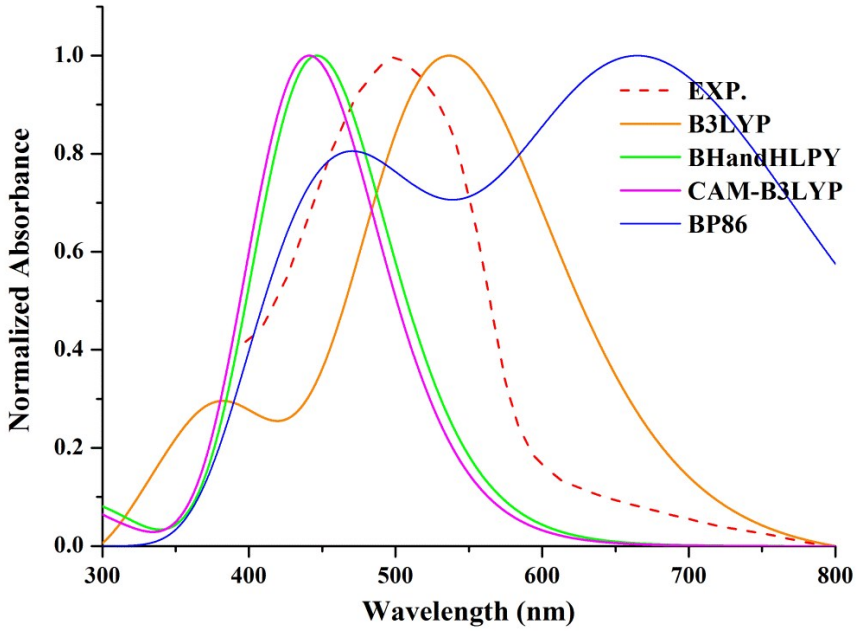

Figure S1. Experimental and simulated absorption spectra for **FENIDT**.

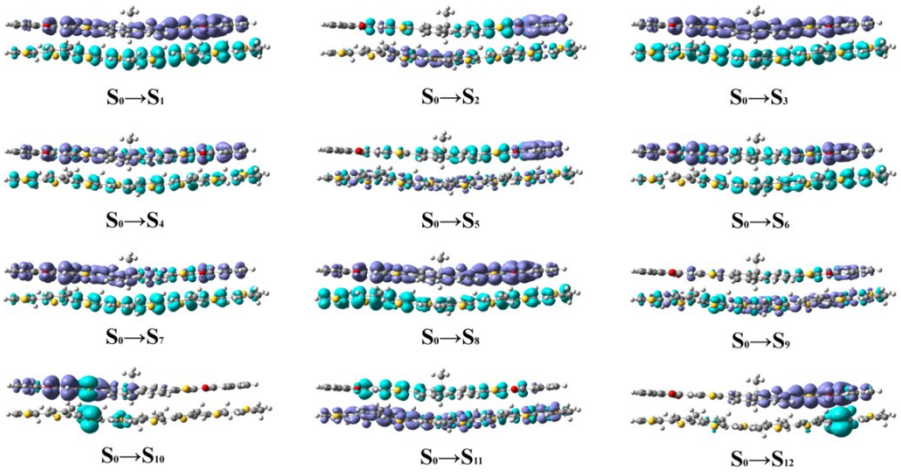

Figure S2. Charge density difference maps for **P3HT/FENIDT** heterojunction obatained at the TD-CAM-B3LYP/6-31G(d, p) level, where the blue and purple colors correspond to the decrease and increase in electron density, respectively.

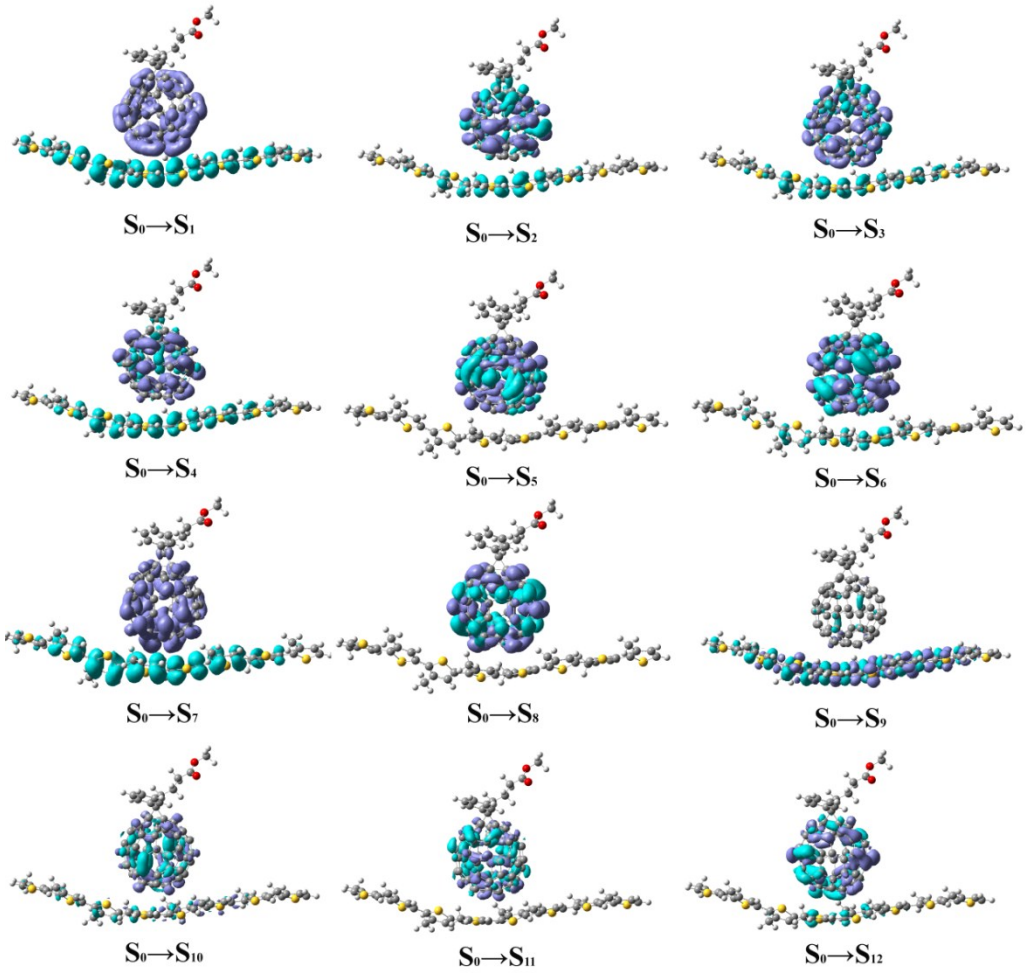

Figure S3. Charge density difference maps for **P3HT/PC_{61}BM** heterojunction obtained at the TD-CAM-B3LYP/6-31G(d, p) level, where the blue and purple colors correspond to the decrease and increase in electron density, respectively.

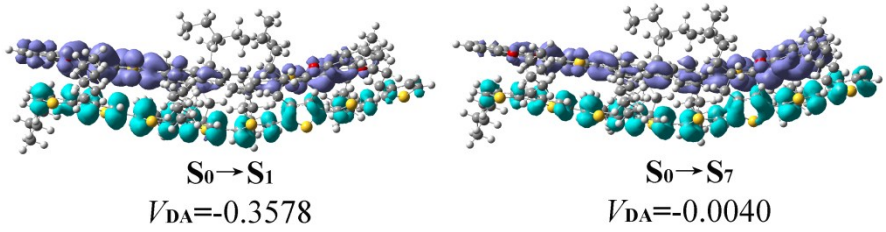

Figure S4. Charge density difference maps and electronic coupling V_{DA} (eV) for interface CT states in **P3HT/FENIDT-style1** interface, where the blue and purple colors correspond to the decrease and increase in electron density, respectively.

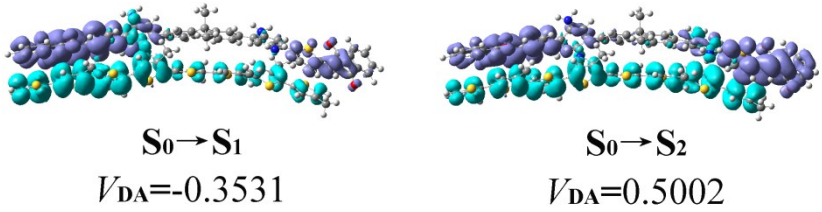

Figure S5. Charge density difference maps and electronic coupling V_{DA} (eV) for interface CT states in **P3HT/3** interface, where the blue and purple colors correspond to the decrease and increase in electron density, respectively.

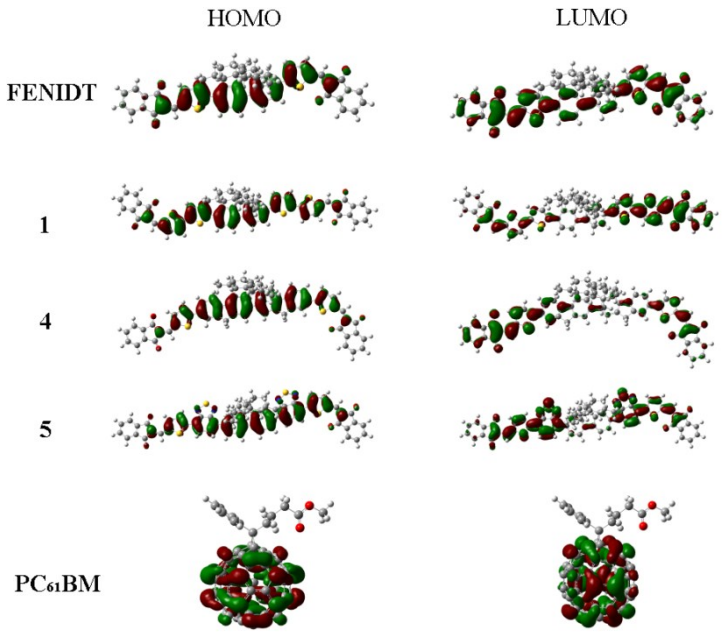

Figure S6. Frontier molecular orbital diagrams for designed molecules **1**, **4** and **5** by B3LYP/6-31G(d, p) calculation.

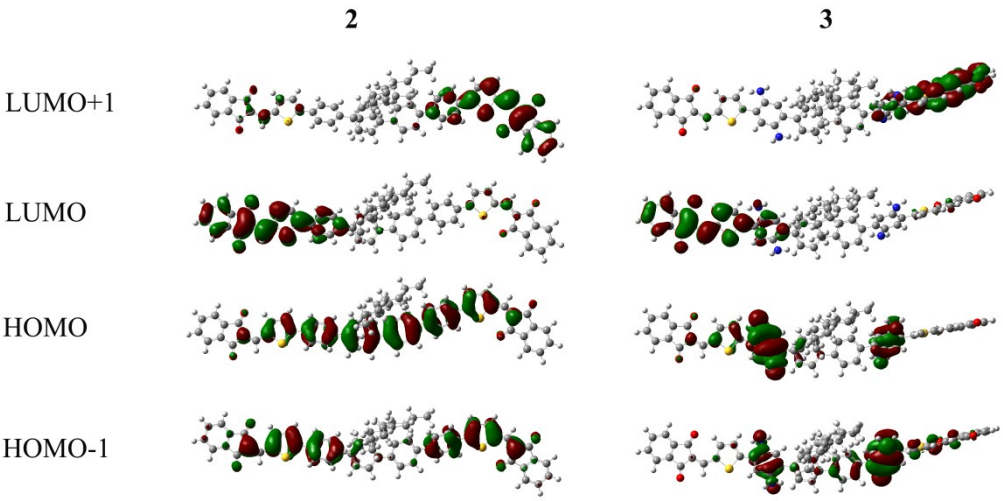

Figure S7. Frontier molecular orbital diagrams for designed molecules **2-3** by B3LYP/6-31G(d, p) calculation.

References

1 Y. Li, T. Pullerits, M. Zhao and M. Sun, *The Journal of Physical Chemistry C*, 2011, **115**, 21865.

2 P. Kjellberg, Z. He and T. Pullerits, *The Journal of Physical Chemistry B*, 2003, **107**, 13737.

3 T. M. Clarke and J. R. Durrant, *Chem. Rev.*, 2010, **110**, 6736.

4 V. Lemaur, M. Steel, D. Beljonne, J.-L. Brédas and J. Cornil, *Journal of the American Chemical Society*, 2005, **127**, 6077.

5 R. A. Marcus, *The Journal of Chemical Physics*, 1956, **24**, 966.

6 Y.-A. Duan, Y. Geng, H.-B. Li, J.-L. Jin, Y. Wu and Z.-M. Su, *Journal of Computational Chemistry*, 2013, **34**, 1611.

7 X. Yang, Q. Li and Z. Shuai, *Nanotechnology*, 2007, **18**, 424029.

8 X. Yang, L. Wang, C. Wang, W. Long and Z. Shuai, *Chemistry of Materials*, 2008, **20**, 3205.

9 R. A. Marcus, *Reviews of Modern Physics*, 1993, **65**, 599.

10 R. A. Marcus and N. Sutin, *Biochimica et Biophysica Acta (BBA) - Reviews on Bioenergetics*, 1985, **811**, 265.

11 P. Siders and R. A. Marcus, *Journal of the American Chemical Society*, 1981, **103**, 748.

12 B. S. Brunschwig, J. Logan, M. D. Newton and N. Sutin, *Journal of the American Chemical Society*, 1980, **102**, 5798.

13 G. R. Hutchison, M. A. Ratner and T. J. Marks, *Journal of the American Chemical Society*, 2005, **127**, 2339.

14 E. F. Valeev, V. Coropceanu, D. A. da Silva Filho, S. Salman and J.-L. Brédas, *Journal of the American Chemical Society*, 2006, **128**, 9882.